



Synthesis of Super Magnetite(Fe_3O_4)/ Bentonite Nanocomposite for Efficient Remediation for Industrial Wastewater Effluents

Asmaa E. Elsayed^{1*}, Doaa I. Osman^{1*}, Sayed K. Attia¹, Hayam M. Ahmed², Eman M. Shoukry², Ghada A. Mahmoud³, Yasser M. Mostafa¹ and Afaf R. Taman¹

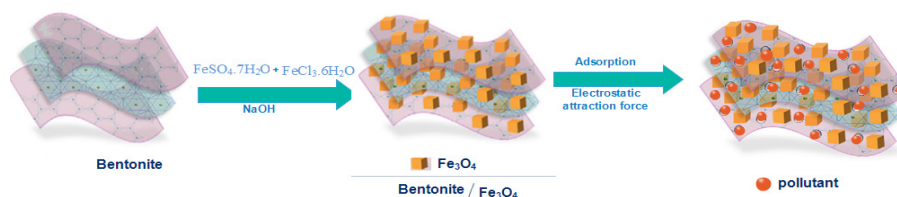
¹Egyptian Petroleum Research Institute, Evaluation and Analysis Department

²Al-Azhar University, Faculty of Science, Chemistry department, Nasr City, Cairo, Egypt

³National Center for Radiation Research and Technology, Atomic Energy Authority, P.O. Box 29, Nasr City, Cairo, Egypt.



Graphical abstract



The goal of the current work was to prepare magnetite/bentonite nanocomposite and testing for expulsion effectiveness of cationic methylene blue (MB) and anionic methyl orange (MO) dyes, phenol and Ni^{2+} from industrial wastewater in individual and combined systems. Batch experiments have been done to observe the best adsorption by altering various parameters such as temperature, pH, the dose of adsorbent, initial pollutants concentration and contact time. The results demonstrated that the optimum pH for removing (MB) was 9.0, (MO) was 4.0, phenol was 7.0 and 4.0 for Ni^{2+} . The optimum concentration, temperature, contact time and adsorbent dose were 100 mg/L, 80 °C, 120 min and 1g of adsorbent, respectively. The sorption process was modeled utilizing Langmuir and Freundlich equations. The adsorption isotherm demonstrated a superior fit to Freundlich than Langmuir equation. The analysis was also modeled using the pseudo-first and second order equations. The pseudo-second-order equation gave better fit with an R^2 value; 0.999 for all pollutants. This implies that our proposed magnetite/bentonite nanocomposite can be utilized as a cheap and excellent adsorbent for expulsion of cationic and anionic dyes, phenol and cationic heavy metal ions from industrial wastewater.

Keyword: Adsorption, Dye removal, Heavy metal ions, Nanocomposite, Wastewater treatment

Introduction

Water contamination is becoming increasingly more serious with the rapid improvement of industries in the world. Numerous sorts of industrial wastewaters have been created and released lately [1]. Among them, dyes, heavy

metal ions, and the phenolic compound. Dyes are a standout amongst the most hazardous materials in industrial effluents [2]. Dyeing effluents created in the dyestuffs, textile, papermaking, leather, and plastics [3,4]. Most of dyes can cause damage to aquatic life and human beings, since they are toxic or carcinogenic [5-7]. Heavy

*Corresponding author e-mail: asmaa.elsayed70@yahoo.com & di_osman@yahoo.com

Received 8 April 2020; Revised 3 May 2020; Accepted 31 May 2020

DOI: 10.21608/ejchem.2020.27520.2574

©2020 National Information and Documentation Center (NIDOC)

metal ions contamination exist in aqueous waste streams from various industries such as metal plating manufacturing, batteries, as well as agricultural sources where fertilizers and fungal sprays are seriously utilized [8]. The release of heavy metal ions into the environment represents a risk to human health additionally to the ecosystem and particularly to people due to the toxicological consequences for living organisms [9,10]. The phenolic compounds are present in the effluents of various industries such as oil refining, petrochemicals, pharmaceuticals, resin manufacturing, plastics, paint, pulp, paper, and wood products [11]. Phenol is toxic to humans and causes headaches, fainting, vertigo and mental disturbance. Additionally, it can cause several severe ecological and environmental problems [12]. Thus, the contamination due to pollutants is extremely dangerous because of their various side effects and carcinogenic nature. Therefore, the significance of water quality protection and improvement is essential in life and expanding continuously [13].

Various techniques have been attempted to treat with those wastewaters including adsorption [14], electrolytic chemical treatment [15], membrane separation [16], chemical reduction [17], and biological treatment [18]. Considering the cost, viability and different impacts, adsorption is a successful and flexible technique to diminish or limit pollutants from water [19]. Activated carbon is generally utilized as adsorbent because of its high adsorption capacity, high surface area, microspores structure and a high surface reactivity. However, there are a few issues, it concerns the high cost and the loss in the regeneration. Therefore, many researchers lean toward a low-cost adsorbent [20].

Clays are belonging to naturally occurring low-cost materials with great adsorption ability [21]. This ability originates from their high specific surface area, chemical and mechanical stability, layered structure and high cation exchange capacity. Bentonite naturally occurring clay is a cheap and a board material that has been utilized as an elective material for the expulsion of dyes [22] and many toxic metal ions [23]. Clays can be modified to improve their sorption ability. One of these adjustment techniques is coating with magnetic particles. The extremely fine size of nano-particles yields favorable characteristics. The reduction in size permits for more atoms are located on the surface of a particle that outcomes

in a remarkable increment in the surface area of Nano powders. This imparts an impressive change in surface morphologies [24]. The novelty of research work is preparation of low cost adsorbent and is applicable to used for removal of different pollutants (organic and inorganic) with high removal efficiency

The objective of the present work is to prepare magnetite/bentonite Nano composite that has been used for the removal of MB and MO dyes moreover phenol and Ni metal ions. Batch adsorption experiments are carried out and the adsorption kinetics and isotherm was contemplated.

Materials and Methods

Materials

Bentonite (average size 200mesh), $\text{FeCl}_3 \cdot 6\text{H}_2\text{O}$ and $\text{FeSO}_4 \cdot 7\text{H}_2\text{O}$, Methyl orange (MO) and Methylene blue (MB) dye were obtained from Siga-Aldrich. For pH adjustment throughout the experiment, hydrochloric acid and/or sodium hydroxide solutions were used as necessary. All chemicals used were reagent grade and were used as received without any further purification.

Preparation of magnetite/ bentonite composite

Natural bentonite is purified by thermal activation process by heating at temperature of 110 °C for 24 h to remove moisture. The bentonite powder was added to aqueous solution containing $\text{FeCl}_3 \cdot 6\text{H}_2\text{O}$ and $\text{FeSO}_4 \cdot 7\text{H}_2\text{O}$ with ratio 2:1. A 0.1 N NaOH was added drop wise to adjust the pH value to 11. Continuously stirring for 2 h at 80 °C until the black particles of magnetite were formed. Then, the solution was filtered and washed with distilled water to remove free sodium hydroxide and become neutral. After that, it was dried in an oven at 100°C for 3 h to afford Fe_3O_4 /bentonite crystals.

Batch adsorption studies

Batch adsorption experiments were carried out. Exactly 25 mL of the contaminated solution of known initial concentration ranged from 15 to 100 mg/L at adjusted pH with a known dose of adsorbent for appropriate time intervals.. After equilibrium attainment, the concentration of samples were determined by UV/VIS spectrometer, model UV-Analytic Jena AG specord 210 plus made by German was used at a wavelength of (190-900) nm at λ_{max} of 664 nm for MB, 464 nm for MO and 270 nm for phenol with a quartz cell of 1.0 cm optical length. The removal percent of samples was calculated using

the following equation [25]:

$$\text{Removal}(\%) = \frac{C_0 - C_t}{C_0} \times 100 \quad (\text{a})$$

where, C_0 (mg/ L) is the initial dye concentration and (C_t) (mg/L) is the concentration at time t .

The adsorption capacity q_e (mg/g) at equilibrium was calculated using the following equation [25]:

$$q_e = \frac{C_i - C_e}{W} \times V \quad (\text{b})$$

where V is the solution volume (L), W is the mass of sample (g), C_e is the equilibrium concentrations (mg/L) .

Results and Discussion

Characterization

Fourier-transform infrared spectroscopy (FT-IR)

FT-IR spectra of bentonite and its magnetic

Nano composite is represented in Fig.(1). It is clear that the characteristics band at 1047 cm^{-1} due to Si-Al-O in plane stretching vibration of layered silicate of nanocomposite confirmed the presence of bentonite. The higher intensity of the bands at 467 cm^{-1} for magnetite/bentonite nanocomposite sited of the magnetite ($\alpha\text{-Fe OOH}$). The bands at 523 cm^{-1} in bentonite and the magnetic one due to the Fe-O deformed however, the intensity of this band is lower in the magnetite/bentonite due to the immobilization by the coating of bentonite.

1-2-X-ray diffraction (XRD)

Figure (2) shows XRD patterns of bentonite and magnetite/bentonite nano-composites. Two strong diffraction peaks for Bentonite (Fig.2a) appeared at 19.787 and 61.944 , which indicate the presence of montmorillonite, a main component of bentonite. The peak at 26.682 corresponds to SiO_2 (Fig.2b) .The broadening of such peak indicates a large number of generated surface defects with high specific surface area and particle distortions which contribute to such diffraction broadening. Which can be indexed to the

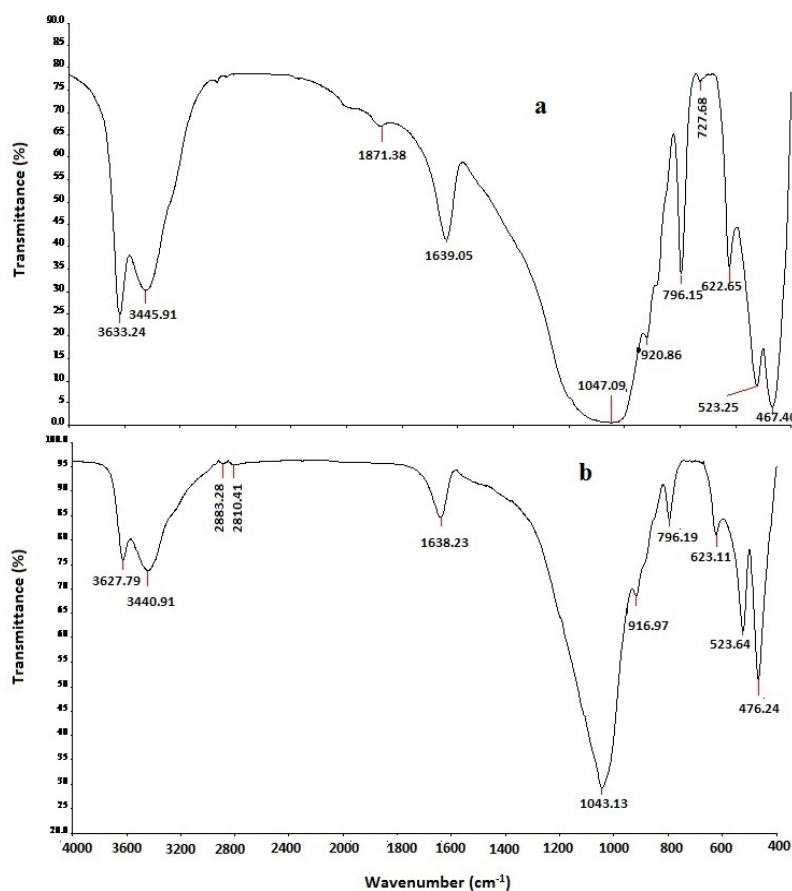


Fig. 1. FTIR of bentonite (a) and magnetite/bentonite nanocomposite (b)

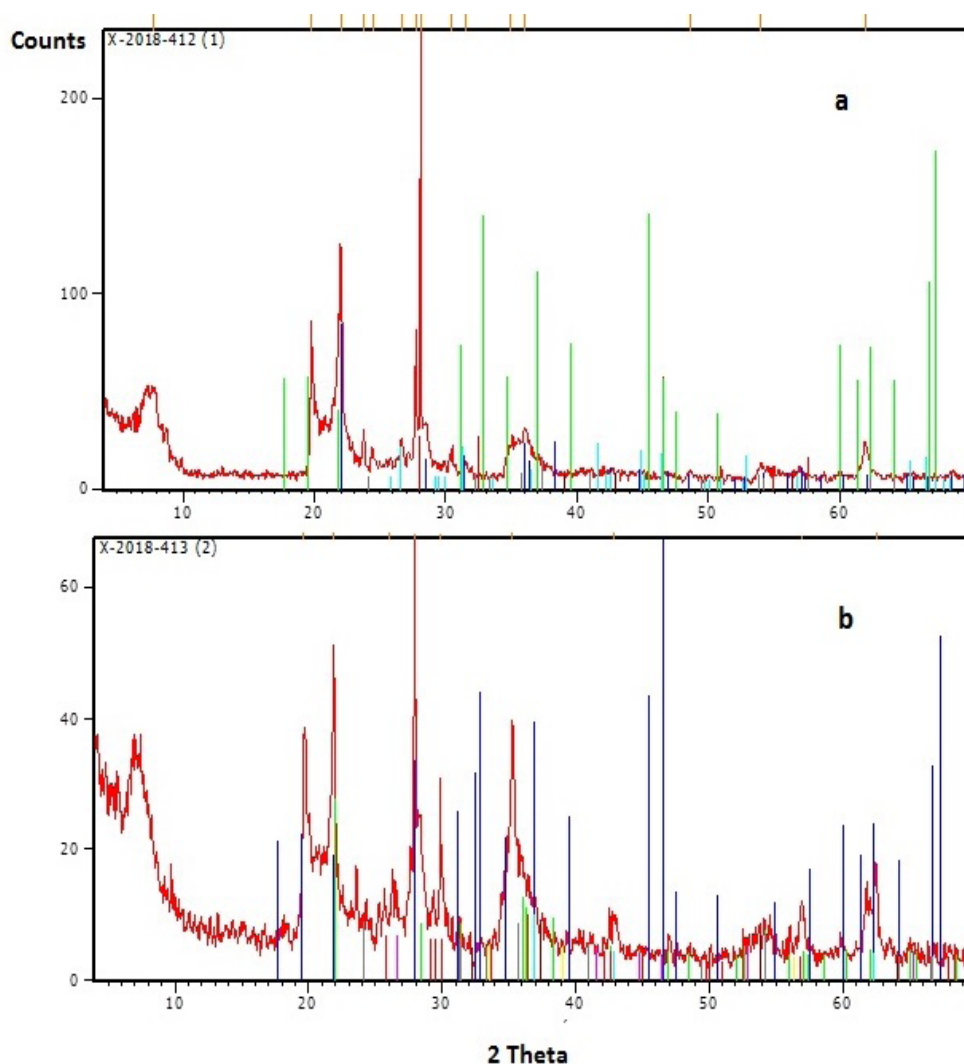


Fig. 2. XRD patterns of bentonite (a) and magnetite/bentonite nanocomposite (b)

planes of Fe_3O_4 (JCPDS 653107). These indicate the successful integration of Fe_3O_4 particles on the surface of bentonite.

SEM

The morphology of natural bentonite and Fe_3O_4 /bentonite nano-composites was studied by SEM, Fig.(3). Very fine micro particles were observed with diameter 0.29-0.91 μm in the SEM of Fe_3O_4 /bentonite nano-composites. Presence of these fine particles leads to increase in the porosity and the surface area of the modified clay. This was confirmed by the measured surface area obtained for modified bentonite ($77.79 \text{ m}^2\text{g}^{-1}$) compared to normal bentonite ($35.77 \text{ m}^2\text{g}^{-1}$)

Specific surface area

The porous properties and pore structure

Egypt. J. Chem. **63**, No. 12 (2020)

of bentonite and magnetite/bentonite nano-composites was investigated by measuring adsorption-desorption isotherms of N_2 using the Brunauer-Emmett-Teller (BET). The surface area and the total pore volume of bentonite and its nanocomposite were determined and were represented in Table (1). It is clear that the value of the specific surface area of bentonite is increased almost twice after modification in the nanocomposite. The meso porous character of the composite was confirmed by the pore size distribution curves as shown in Fig. (4) due to pore diameter (DV) for the bentonite and its nanocomposite increased from 18.26 nm to 38.16 nm. and in the range 2-50 nm so followed IV type isotherm curve .

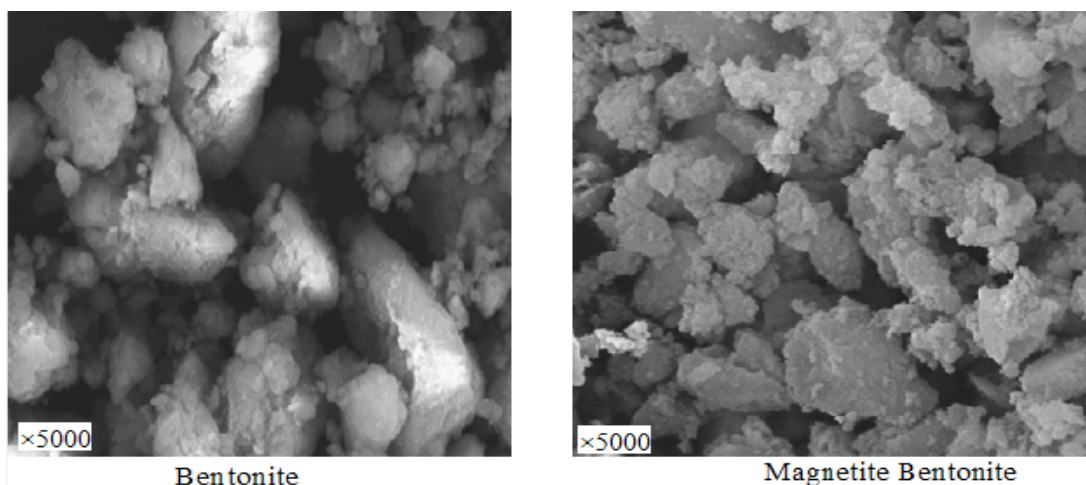


Fig.3. SEM of bentonite (a) and magnetite bentonite (2)

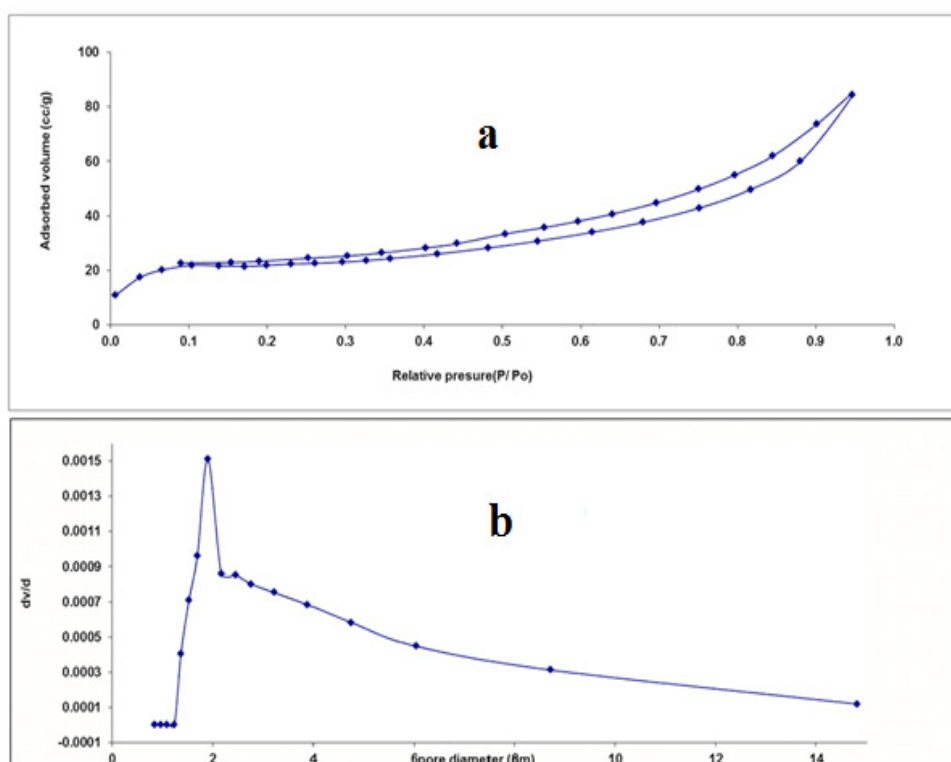


Fig.4. Nitrogen adsorption –desorption isotherm and pore size distributions for magnetite bentonite.

TABLE 1. Physical properties of bentonite and magnetite/bentonite nanocomposite

Type of Clay	Specific Surface area, S (BET) (m^2/g)	Pore volume, VP (cc/g)	Pore diameter, DV (nm)
Bentonite	35.77	0.1633	18.26
Magnetite / bentonite	77.79	0.1307	38.16

Thermogravimetric analysis (TGA)

The bentonite and magnetite/bentonite nanocomposite were characterized by TGA as shown in Fig. (5). It can be observed that the total weight loss was 9.681% and 9.546% for bentonite and its magnetite nanocomposite, respectively. It is clear that the magnetite/bentonite nanocomposite showed a reduction in the starting weight loss temperature (310°C) however expanding in the highest weight loss temperature (840°C) and decreasing in the maximum weight loss rate as compared with bentonite. This may be due to the presence of magnetite resulting in an increase in the diffusion path of oxygen. This phenomenon demonstrates that the addition of magnetite to bentonite which increases its thermal stability.

Magnetization analysis

The magnetic behavior of magnetite/bentonite nanocomposite was studied by recording

magnetization (M) against applied magnetic field (G) at room temperature using VSM. The saturation magnetization was 5.8 emu/g which was sufficient magnetic separation.

Adsorption capacity of magnetite/bentonite nanocomposite

The adsorption of pollutants cationic (methylene blue MB) and anionic methyl orange MO), phenol and nickel ions from aqueous solutions onto magnetite/bentonite nanocomposite at different solution pH, adsorbent dose (nanocomposite) and initial pollutants concentration and temperatures has been studied.

Effect of solution pH

The adsorption of magnetite/bentonite nanocomposite was investigated onto the different investigated pollutants over three pH values, 4, 7, and 9, as shown in Fig. (7). It can be noticed

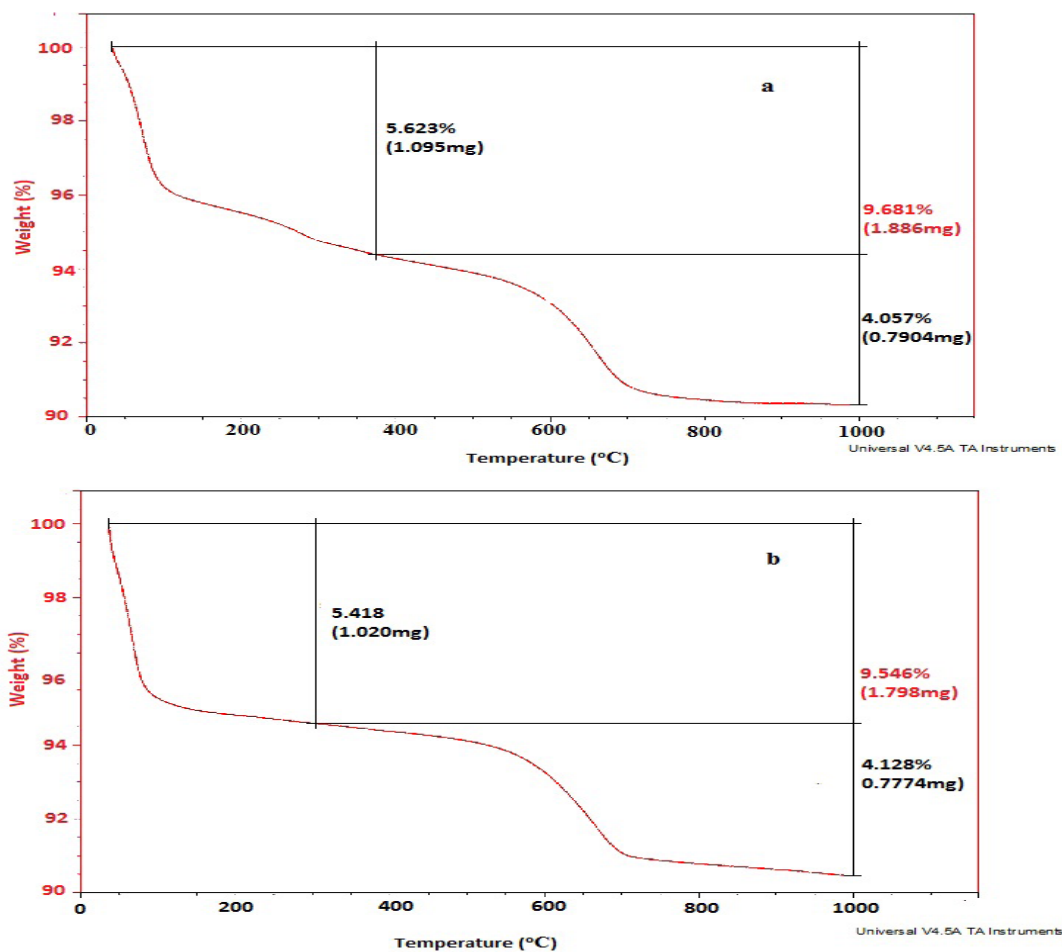


Fig.5. TGA thermograms of bentonite (a) and magnetite/bentonite nanocomposite (b)

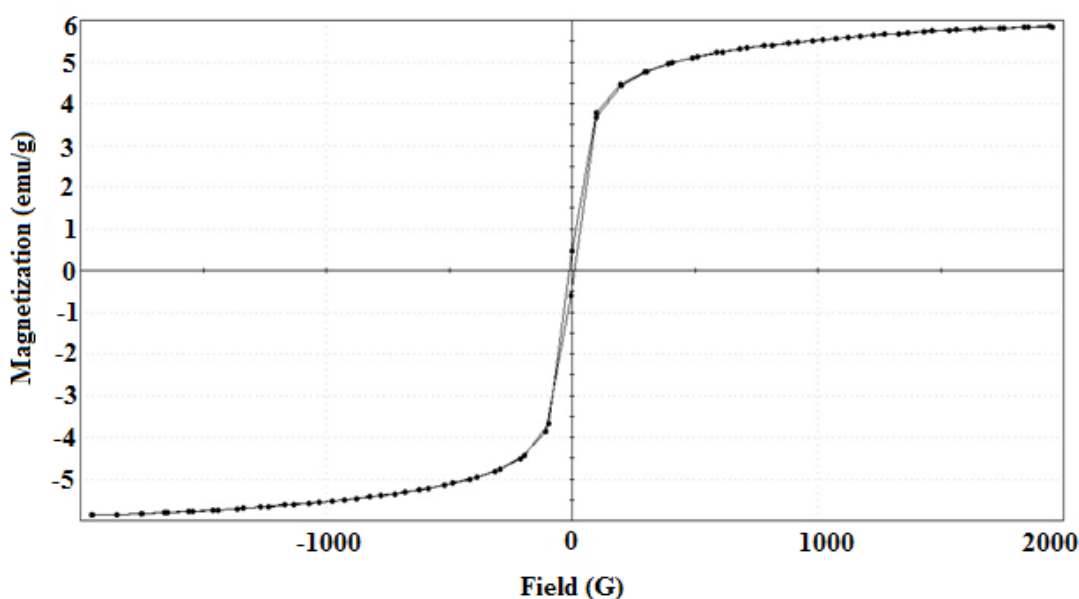


Fig.6. Magnetization of magnetite/bentonite nanocomposite

that, the removal percent of MB increased with the increase in pH values due to an electrostatic attraction was done between the MB cations and negative charge of the nanocomposite. On the other hand, the removal of MO from solution decreased with increasing pH from 4 to 9.0, respectively, this is due to that a pH 4 a strong interaction between the negatively charge on the dye and positively charge on the nanocomposite. Consequently, a repulsion between anions with the negative charge on the nanocomposite was done at higher pH,9, that was responsible of decreasing in the removal percent.

In case of the phenol (Ph) the removal percent increased with increasing of pH from 4.0 to 7.0 followed by a sharp decrease in the removal percent was observed with the increase of pH value to 9.0. This means the maximum removal percent performed, at pH value 7.0. It can be noticed that Acceptable removal was obtained at low pH value 4 due to at higher pH value e more OH^- ions are presented in the solution that competes Ph to the active sites in the nanocomposite resulting in the reduction of the phenol removal percent.

The removal percent of Ni^{2+} decreased with increasing the pH value where it got the maximum removal value at pH (4.0) followed by a sharp decrease in the removal percent. This is due to the Ni salt solution is precipitated as Ni hydroxide which has no effect on the removal percent.

Effect of adsorbent dose

Figure (8) shows the effect of magnetite/bentonite nanocomposite on the removal of the investigated pollutants, MB, MO, phenol, and Ni^{2+} , from the aqueous solutions. The results indicated that the increase in the dosage of the nanocomposite accompanied by a faster increase in the percentage of removal of pollutants. This is due to the removal efficiency is not linearly increased presumably. At high adsorbent dose, an aggregation of the nanocomposite was done as well as a reduction in surface area was obtained which in turn reduced the active sites of the adsorbent. This means an accumulation of pollutants in the vacant active sites on the surface of the nanocomposite. The results indicated that the nanocomposite is highly efficient in pollutants removal as only a small quantity is required to achieve an excellent performance.

Effect of contact time

The effect of contact time on the removal of MB, MO, Ph and Ni^{2+} was shown in Fig. (9). It is observed that by increasing the contact time, the removal efficiently increased until reach its maximum value. At the initial stage of the contact time, the adsorption of pollutants on the adsorbent (composite) are fast. This is due to the high diffusion of pollutants molecules into the large external surface area of the composite also to large number of vacant active sites which are available. After the equilibrium adsorption, the

available adsorption sites become fewer due to the repulsions occurred between pollutant molecules on composite surface that impendent the adsorption process. It is clear that the percent of removal of MB is higher than the other pollutants. This is due to the strong electrostatic attraction between the negative charge of composite and the positive charged cationic dye (MB).

Adsorption kinetics

In order to understand the process of adsorptions, two kinetic models were applied to the experimental data.

The linear from of the pseudo -first-order kinetic model is expressed by equation.

$$\ln(q_e - q_t) = \ln q_e - Kt \quad (1)$$

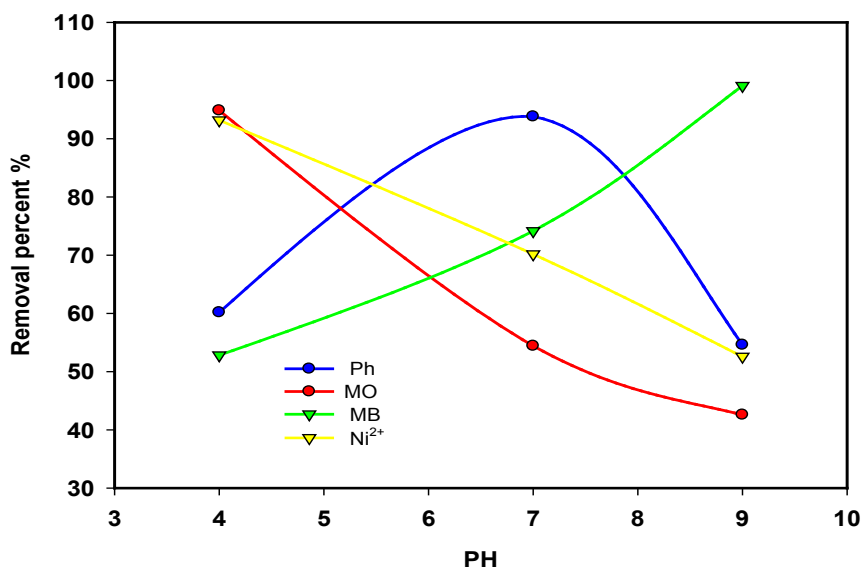


Fig.7. Effect of medium pH on removal percent of pollutants at initial concentration;100 ppm , nanocomposite dose;1 g, Temperature;100 °C, and contact time;120 min.

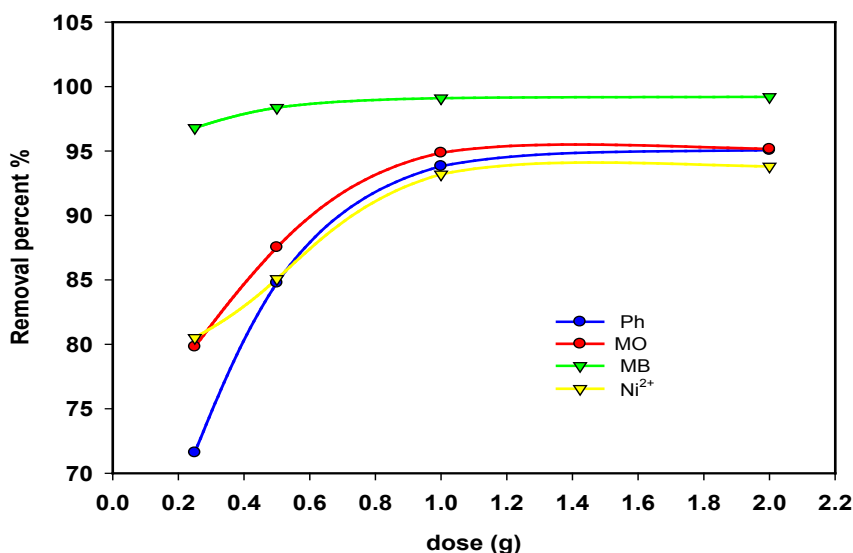


Fig.8. Effect of adsorbent dose on removal percent of pollutants at initial concentration; 100ppm, medium pH; 4for (Ni²⁺,MO), 9for(MB), 7for(Ph) Temperature;80°C, and contact time;120mint.

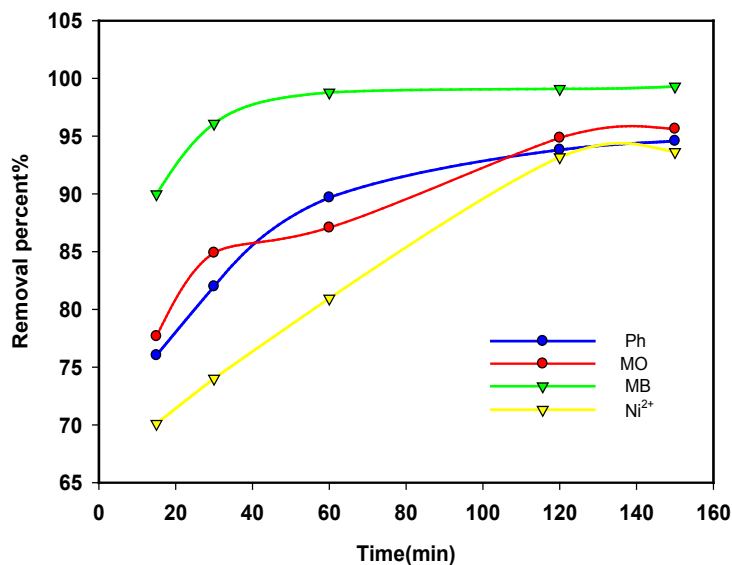


Fig. 9. Effect of contact time on removal percent of pollutants at initial concentration;100ppm , medium pH;4for(Ni²⁺,MO), 9for(MB),7for(Ph) Temperature;80°C, and adsorbent dose;1g.

where q_e (mg/g) is the concentration of pollutant adsorbed at equilibrium, q_t (mg/g) is the concentration of pollutant at time t and K (min⁻¹) is the pseudo-first order constant.

The pseudo-second order rate equation in the linear form is expressed as :

$$\frac{1}{q_t} = \frac{1}{Kq_e^2} + \frac{1}{q_e} \quad (2)$$

where K (g mg⁻¹ min⁻¹) is the pseudo-second order rate constant.

The results of the pseudo-first order model (Eq.1) and for the pseudo-second order model (Eq.2) are represented in Fig.(10) and the obtained data are shown in Table (2). It was found that the magnetite/bentonite nanocomposite gave a good affinity to remove the pollutants from aqueous solutions. The best-fit model was determined depending on the linear correlation coefficient R^2 . According to the values of the correlation coefficients, the pseudo-second order rate model nearly to the unity and larger than the pseudo-first order for all investigated systems as shown in Table (2). This means the adsorption kinetic process was described by the pseudo-second-order model very well. It was followed by the diffusion of the pollutant molecules from the bulk of the solution to the external surface and the pore structure of the magnetite/ bentonite nanocomposite.

Effect of pollutants initial concentrations

The effect of initial concentrations of MB, MO, Ph and Ni²⁺ was studied as represent in Fig. (11). The results pointed to that as the initial concentrations of the pollutants increased the removal percent decreased.

At low concentration of pollutants, most pollutants in the solution might contact with the active sites of the adsorbent and as the concentration was increased, all pollutant species would not be available to contact with active surface due to active sites are already filled up so that the removal percent of pollutants decreased at high concentrations as shown in Fig. (11).

Analysis of the isotherm data

Analysis of such isotherm data is important in order to develop the equation which represents the results and give indication about the adsorption capacity. In this study two isotherms were selected, Langmuir and Freundlich equations.

Langmuir isotherm

It is represented by the model:

$$\frac{C_e}{q_e} = \frac{1}{K_L} + \frac{a_L}{K_L} C_e \quad (3)$$

Where C_e is the equilibrium concentration of the adsorbate (mg/L), K_L and a_L are constants.

By plotting C_e/q_e against C_e for different adsorbate, MB, MO, Ph and Ni²⁺, as shown in Fig. (9). A series of straight lines have been obtained which indicated that the adsorption process

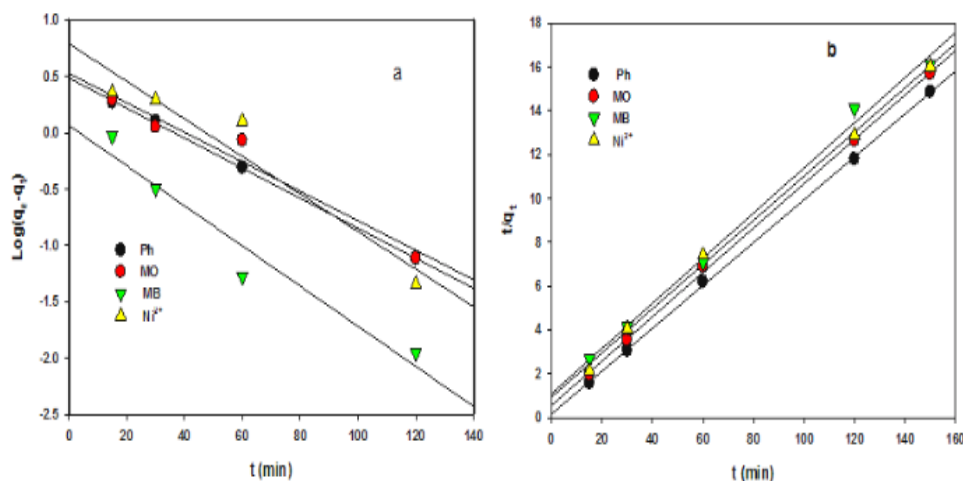


Fig. 10. Adsorption kinetic plots of the pseudo first order (a) and the pseudo second order (b) models

TABLE 2. Parameter of the pseudo first order and the pseudo second order

The kinetic model	parameter	Ph	MO	MB	Ni ²⁺
Pseudo first order	$q_{e^{exp}}$ (mg/g)	8.7479	9.2499	13.56	11.7479
	k_1 (min ⁻¹) $\times 10^{-3}$	0.0301	0.0301	0.0410	0.0383
	$q_{e^{ca}}$ (mg/g)	3.0521	3.3356	7.1573	6.1483
	R ²	0.9951	0.9563	0.9452	0.9226
Pseudo second order	k_2 (g/ mg min)	0.2991	0.0185	0.1975	0.0108
	$q_{e^{cal}}$ (mg/g)	1.0235	9.8823	9.7082	9.9235
	R ²	0.9964	0.9931	0.9954	0.9976

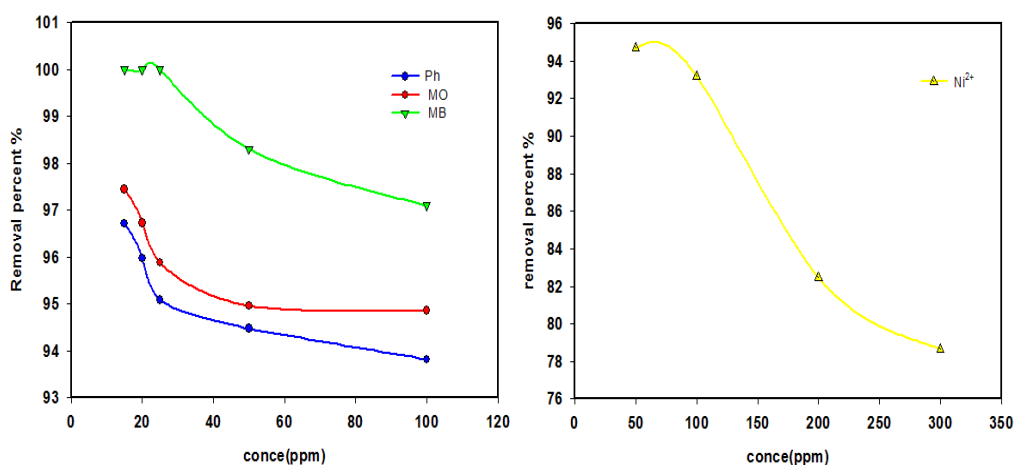


Fig.11. Effect of initial concentration on removal percent of pollutants at contact time;120mint.,mediu mpH;4for(Ni²⁺,MO),9for(MB),7for(Ph) Temperature;80°C, and adsorbent dose;1g.

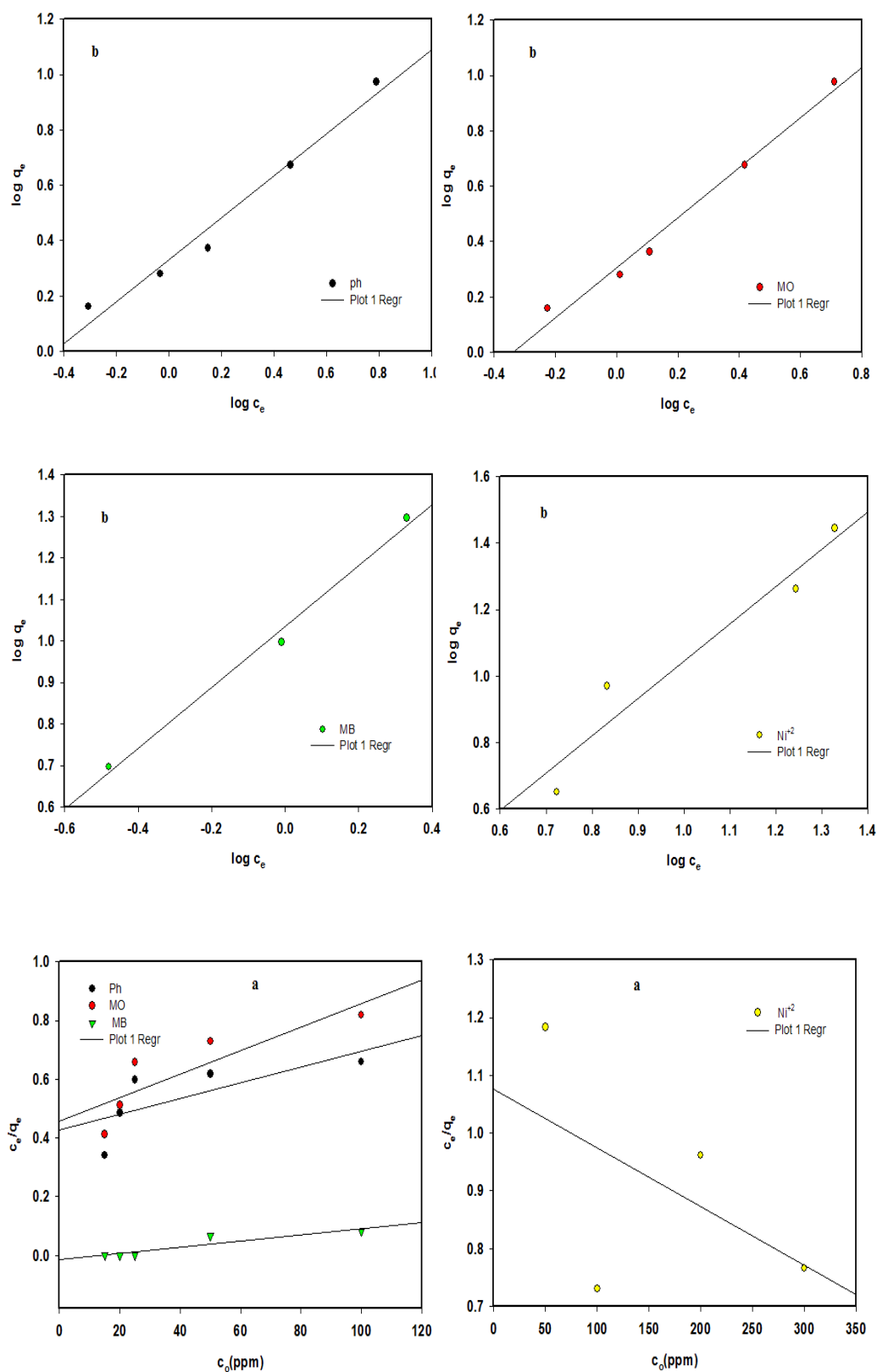


Fig.12. Adsorption Langmuir isotherm(a) Adsorption Freundlich isotherm(b)

confirmed with the Langmuir adsorption. The slopes (a_L/K_L) and intercepts ($1/K_L$) of these straight lines. The values of (a_L/K_L) corresponding to the maximum adsorption capacity of the magnetite/bentonite nanocomposite. Langmuir parameter, K_L , a_L and maximum adsorption capacity have calculated and are represented in Table (3). It is clear that MB have a higher adsorption capacity (13.56 mg/g) followed by Nickel salt, MO and the phenol compound.

Freundlich isotherm:

The experimental equilibrium data for the adsorption of pollutant onto magnetite/bentonite nanocomposite have been analyzed using the linear form freundlich isotherm as given by the equation:

$$\text{Log } q_e = \text{log } K_f + (1/n) \text{log } C_e \quad (4)$$

The experimental results have been plotted as $\text{log } q_e$ against to C_e , where a group of straight lines have been obtained as shown in Fig.(10) The freundlich parameters, K_f and n , for the adsorption of pollutants onto the magnetite bentonite composite have, calculated using the least-square method and are tabulated in Table (3). The results indicated that the values of Freundlich exponent, n are greater than unity except of Ni^{2+} (0.8889) indicated that the adsorption of pollutants are favorable by adsorption. The correlation coefficients (R^2) were higher than 0.93 for all investigated systems suggested that the adsorption of pollutants onto the composite belonged typical multi-molecular adsorption. This means that sorption of pollutant is heterogeneous energy distribution. The isotherm study explained that the adsorption data are well described by the Freundlich model.

Effect of temperature

To understand the effect of temperature on the adsorption process the pollutants, MB, MO, Ph and Ni^{2+} , adsorption experiments were performed at three different temperature 30, 60 and 80°C. The results are represented in Fig. (13). It was observed that the removal percent of the pollutants increased with increasing the temperature. This is due to that the raising of temperature increased the kinetic energy of the molecules which enhanced at the contact surface between the nano composite adsorbent and adsorbate pollutants. The increase of temperature would increase the adsorption capacity implied that the adsorption representing an endothermic process.

Thermodynamic of adsorption

The standard free energy change (ΔG° , KJ/mol), the standard enthalpy change (ΔH° , KJ/mole) and the standard entropy change (ΔS° , J/mol/k) of the adsorption isotherms at various temperatures were studied. The vales of ΔG° , ΔH° and ΔS° are obtained from the following equations.

$$\Delta G^\circ = -RT \ln K \quad (5)$$

$$\ln K = \frac{\Delta S^\circ}{R} - \frac{\Delta H^\circ}{RT} \quad (6)$$

Where R is the gas constant = 8.314J/mol K, K is the distribution coefficient, and T is Temperature in Kelvin

Figure (14) represents the plot of $\ln k$ against $1/T$ and the calculated thermodynamic parameters ΔG° , ΔH° and ΔS° are shown in Table (4). The positive values of ΔG° confirmed that the adsorption of pollutants onto the magnetite/bentonite nanocomp osite is spontaneous. The absolute value of ΔG° increased with rising temperature indicated that the higher temperature

TABLE 3. Parameters of Langmuir and Freundlich isotherm models

Model	parameter	Ph	MO	MB	Ni^{2+}
Langmuir	$K_a(\text{L/mg}) \times 10^{-3}$	6.24	8.7461	10.657	6.2408
	R_L	1.6×10^{-3}	1.14×10^{-3}	1.415×10^{-4}	1.599×10^{-3}
	R^2	0.5279	0.7367	0.8347	0.52797
Freundlich	$K_f[\text{mg/g}(\text{mg/L})^{-(1/n)}]$	2.1429	2.0232	10.8455	8.3174
	$1/n$	0.7574	0.90234	0.73435	1.12499
	n	1.3203	1.10822	1.3617	0.8889
	R^2	0.9733	0.9837	0.9915	0.93425

facilitated the endothermic adsorption. This is due to increasing the mobility of adsorbate molecules in other words it depends mainly on the movement of adsorbate. The positive value of ΔH (4.7-7.7 KJ/mole) suggested the adsorption process would be

endothermic reaction. The positive values of ΔS° (5.4-20.2 J mole⁻¹K⁻¹) indicated the adsorption is an entropic increasing randomness at the solid/liquid interface during the adsorption.

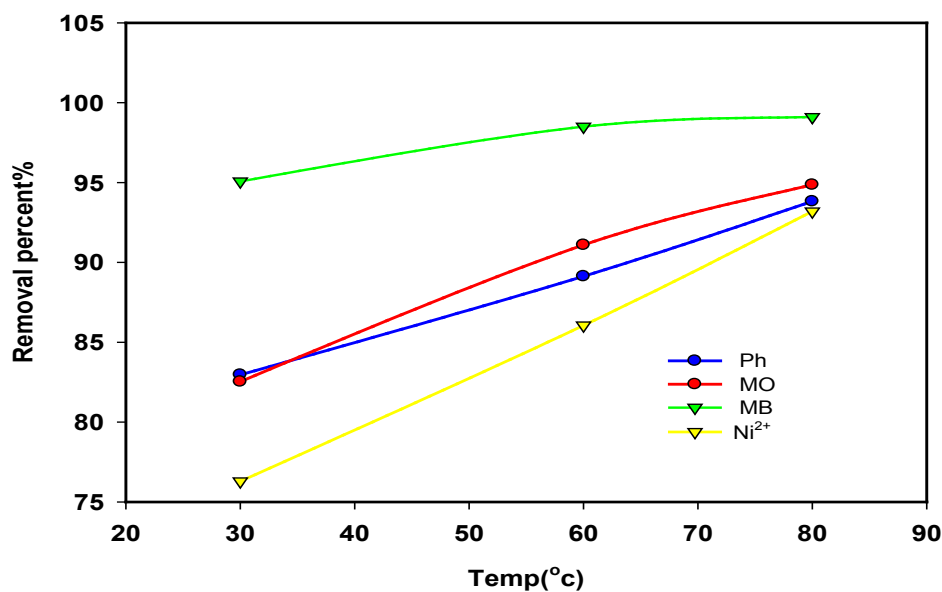


Fig.13. Effect of temperature on the removal percent of pollutants at initial concentration;100ppm, at contact time;120mint.,mediumpH;4for(Ni²⁺,MO),9for(MB),7for(Ph) and adsorbent dose;1g.

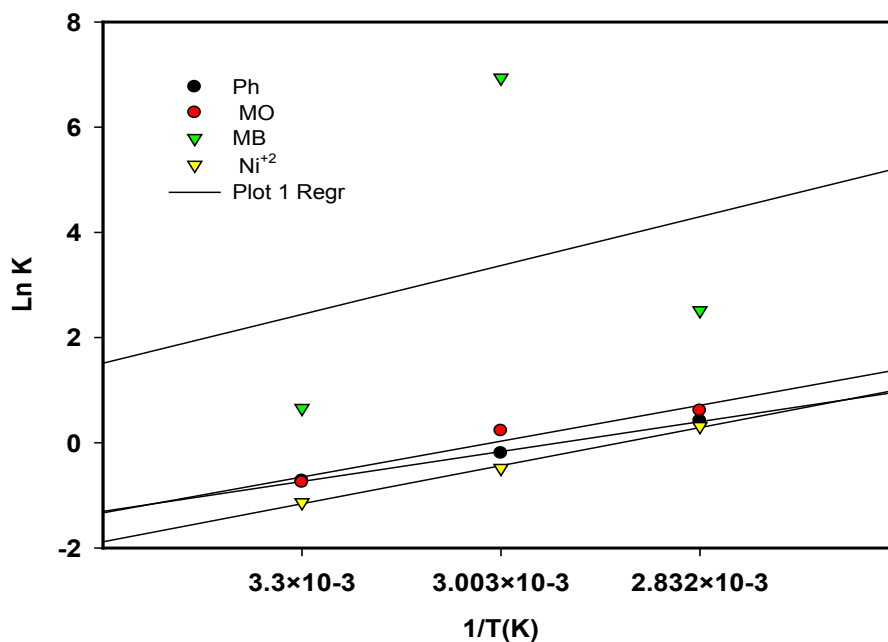


Fig.14. Thermodynamic of adsorption process of different pollutants

TABLE 4. Thermodynamic parameter of adsorption process of different pollutants

pollutants	Temperature (K)	G° Δ (KJmol ⁻¹)	S°Δ (K ⁻¹ J mol ⁻¹)	H°Δ (KJ mol ⁻¹)	R ²
Ph	303	-1855	6108	4724	0.9977
	333	-2029			
	353	-2151			
MO	303	-1633	5408	5664	0.94001
	333	-1795			
	353	-1903			
MB	303	-6139	2028	7721	0.9828
	333	-6748			
	353	-7154			
Ni ²⁺	303	-2100	6953	6018	0.96637
	333	-2309			
	353	-2448			

Desorption process for different adsorbent materials

From the economic point of view, the adsorbent could be recycled therefore, regeneration of the adsorbent and reuse of the adsorbed species are significant aspects in a successful adsorption process, especially that there is strong emphasis on waste removal, recovery and reuse. Adsorbents that are characterized by better regeneration and better recovery capacity for pollutants (dyes, metal and phenol) are desirable from the cost of usage and recovery of valuable pollutants points of view. The (MB and Ni²⁺ ions) and (MO and Ph) adsorbed onto the magnetite bentonite could be easily desorbed from the adsorbent by diluted HCl and NaOH solution respectively to recover

MB, Ni²⁺, MO and Ph. The sorption/desorption cycle was repeated for the desired number of cycles until pollutants sorption capacity was less than 50 % of the sorbed pollutant in the first cycle.

Fig. (15) show the adsorption capacity percent recovery of magnetite bentonite which desorbed or regenerated for 4 consecutive cycles. It is clear from Fig.(15) that the adsorption capacity of the adsorbent decreases with the consecutive repeating of the adsorption–desorption cycles. This means decrease in the percent recovery of the adsorbents adsorption capacity by consecutive regeneration cycles due to the unavoidable losing weight of adsorbent during desorption process as shown in Fig.

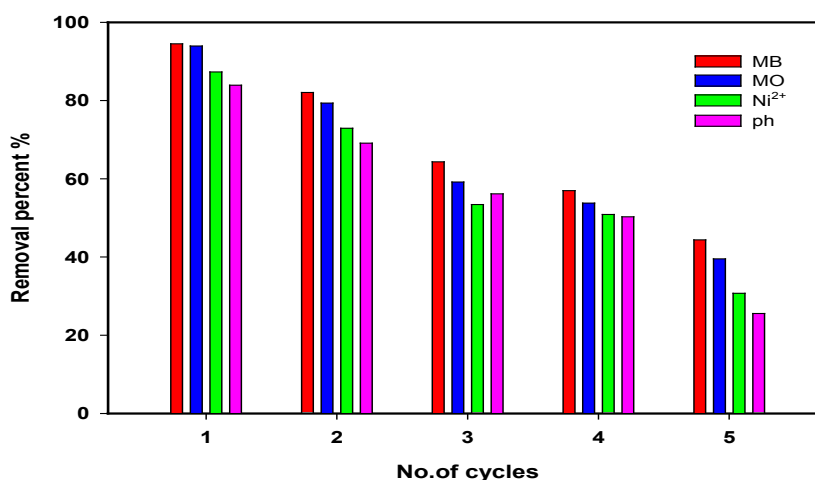


Fig .15. Effect of adsorption –desorption cycles on adsorption capacities of Magnetite bentonite in the removal of all pollutants from waste water

Conclusion

- 1- Optimum conditions for adsorption are time 120 min, concentration 100 ppm, temperature 80°C, dose 1 g and pH4 for MO and pH9 for MB
- 2- Adsorption of MB more than MO
- 3- Adsorption of MB&MO in combined system accordance to adsorption in single system
- 4- The sorption process is according to Freundlich equation and second order reaction
- 5- Adsorbent can be regenerated and reused four times.

References

1. Fu, F., Wang, Q., Removal of heavy metal ions from wastewaters: a review. *J. Environ. Manage* **92**, 2011, 407- 418.
2. Pokhrel, D., Viraraghavan, T., Treatment of pulp and paper mill wastewater-a review. *Sci. Total Environ.* **333**, 2004, 37-58.
3. Reddy, D.H., Lee, S.M., Application of magnetic chitosan composites for the removal of toxic metal and dyes from aqueous solutions. *Adv. Colloid Interface Sci.* **201-202**, 2013, 68-93.
4. A. El-Hag Ali, A. I. Raafat, G. A. Mahmoud, N.A. Badway, M. A. El-Mottaleb, M. F. Elshahawy, Photocatalytic Decolorization of Dye Effluent Using Radiation Developed Polymeric Nanocomposites. *Journal of Inorganic and Organometallic Polymers and Materials.* **26**, *3*, 2016,606–615.
5. G. A. Mahmoud, S. E. Abdel-Aal, N. A. Badway, A. A. Elbayaa, D. F. Ahmed, A novel hydrogel based on agricultural waste for removal of hazardous dyes from aqueous solution and reuse process in a secondary adsorption, *Polym. Bull.* **74**: 2017, 337–358.
6. S. E. Abdel-Aal, G. A. Mahmoud, A.A. Elbayaa, N. A. Badway, D. F. Ahmed, Consecutive Removal of Hazardous Dyes from Aqueous Solutions by Composite hydrogels Based on Rice Straw, *Journal of Research Updates in Polymer Science*, **6**, 2017,102-117.
7. G. A. Mahmoud, S. E. Abdel-Aal, N. A. Badway, S. A. Abo Farha, E. A. Alshafei, Radiation synthesis and characterization of starch-based hydrogels for removal of acid dye. *Starch/Stärke* **65**, 2013,1–9.
8. Wan, M. W., Kan, C. C., Buenda, D. R., & Maria, L. P.D. Adsorption of copper(II) and lead(II) ions from aqueous solution on chitosan-coated sand. *Carbohydrate Polymers*, **80**, 2010, 891–899.
9. G. A. Mahmoud, Adsorption of copper(II), lead(II), cadmium(II) ions from aqueous solution by using hydrogel with magnetic properties, *Monatsh. Chem.* **144**, 2013, 1097–1106.
10. G. A. Mahmoud, E. A. Hegazy, N. A. Badway, K. M. M. Salam, S. M. Elbakery, Radiation synthesis of imprinted hydrogels for selective metal ions adsorption, *Desalination and water treatment*, **57**, *35*, 2016, 16540-16551.
11. R.D. Vidic, C.H. Tessmer, L.J. Uranowski, Impact of surface properties of activated carbons on oxidative coupling of phenolic compounds, *Carbon* **35**, *9*, 1997, 1349–1359.
12. I. Abou El Fadl, G. A. Mahmoud, N. A. Badawy, F. H. Kamal, A.A. Mohamed Pectin-based hydrogels and its ferrite nano composites for removal of nitro compounds. *Desalination and Water Treatment*, **90**, 2017, 283–293.
13. Yang, M., A current global view of environmental and occupational cancers. *J. Environ. Sci. Health Part. C* **29**, 2011, 223-249.
14. Gupta, V.K., Suhas, Application of low-cost adsorbents for dye removal a review. *J. Environ. Manage* **90**, 2009, 2313-2342.
15. Xing, Y., Chen, X., Wang, D., Electrically regenerated ion exchange for removal and recovery of Cr (VI) from wastewater. *Environ. Sci. Technol.* **41**, 2007, 1439-1443.
16. Dasgupta, J., Sikder, J., Chakraborty, S., Curcio, S., Drioli, E., Remediation of textile effluents by membrane based treatment techniques: a state of the art review. *J. Environ. Manage* **147**, 2015, 55-72.
17. Vadahanambi, Lee, Kim, Oh, "Arsenic removal from contaminated water using three-dimensional graphene-carbon nanotube-iron oxide nanostructures", *Environ.Sci. Technol*, **47**, 2013, 10510–10517.
18. Herrero, M., Stuckey, D.C., Bioaugmentation and its application in waste water treatment: a review. *Chemosphere* **140**, 2015, 119-128.
19. Yan, H., Yang, L.Y., Yang, Z., Yang, H., Li, A.M., Cheng, R.S., Preparation of chitosan/poly (acrylic acid) magnetic composite microspheres and

- applications in the removal of copper (II) ions from aqueous solutions. *J. Hazard. Mater* **229**, 2012,371-380.
20. Hassan AF, Abdel-Mohsen AM, Fouda MMG, Comparative study of calcium alginate, activated carbon, and their composite beads on methylene blue adsorption, *Carbohydrate Polymers*. **102**, 2014,192-198.
 21. Y. Liu, Y. Kang, B. Mu, and A. Wang, "Attapulgit/bentonite interactions formethylene blue adsorption characteristics from aqueous solution," *Chemical Engineering Journal*, vol. **237**, 2014,403–410.
 22. F. Bergaya, B.K.G. Theng, G. Lagaly, Handbook of Clay Science , Elsevier, Oxford UK (2006)
 23. Mobasherpour, I., Salahi, E. & Pazouki, M. , Removal of nickel (II) from aqueous solutions by using nano-crystalline calcium hydroxyapatite, *J. Saudi. Chem. Soc.* **15**, 2011, 105-112.
 24. G. A. Mahmoud, S. E. Abdel-Aal, N. A. Badway, A. A. Elbayaa, D. F. Ahmed, A novel hydrogel based on agricultural waste for removal of hazardous dyes from aqueous solution and reuse process in a secondary adsorption, *Polym. Bull.* **74**, 2017 ,337–358.
 25. Zhuang Li, Lan Li, Danling Hu, Chao Gao, Jinyan Xiong, Huiyu Jiang , Wei Li, Efficient removal of heavy metal ions and organic dyes with cucurbit [8]uril-functionalized chitosan, *Journal of Colloid and Interface Science* **539** , 2019,400–413.